ISSN: 2639-7536

Research Article

Petroleum and Chemical Industry International

Comparative Study of Corrosion, Mechanical and Electrical Characteristics of Tungsten inert Gas and Friction Stir Welded Joints

Bhardwaj Kulkarni[1*], Sandeep Pankade[2]

[1]*Chamber of Marathwada Industries and Agriculture, Cluster Development Cell, Aurangabad, Maharashtra, India.*

[2]*Maharashtra Institute of Technology, Department of Mechanical Engineering, Aurangabad, Maharashtra, India.*

[*]Corresponding Author
Bhardwaj Kulkarni, Chamber of Marathwada Industries and Agriculture, Cluster Development Cell, Aurangabad, Maharashtra, India.

Submitted: 27 Mar 2023; **Accepted:** 06 April 2023; **Published:** 12 Apr 2023

Citation: Kulkarni, B., Pankade, S. (2023). Comparative Study of Corrosion, Mechanical and Electrical Characteristics of Tungsten inert Gas and Friction Stir Welded Joints. *Petro Chem Indus Intern, 6*(2), 40-48.

Abstract

Aluminium alloys are welded using both tungsten inert gas welding (TIG) and friction stir welding (FSW). FSW doesn't need any filler material and shielding gas which results in reduced degradation of the environment. In the present study, joints with FSW and TIG processes were compared in terms of microstructure, corrosion resistance, mechanical, and electrical properties. With a microstructural study, the average grain size of various regions was determined. Coarse grain increases the rate of exfoliation corrosion. The fine grain structure in the FSW stir zone increases the hardness. The coarse grains are a prerequisite for enhanced electrical conductivity. The coarse grains in the heat-affected zone and thermomechanically affected zones of FSW joints result in increased electrical conductivity. In the case of friction stir welded joints, there is an inverse relationship between hardness and electrical conductivity. As hardness increases, electrical conductivity decreases, and vice versa. Hence, in the case of FSW hardness test can be substituted by an electrical conductivity test. In the case of TIG, no relation was found between hardness and electrical conductivity. High Silicon content at the weld region of TIG significantly reduces electrical conductivity.

Keywords: Exfoliation Corrosion, Friction Stir Welding (FSW), Tungsten Inert Gas Welding (TIG), Microstructure, Mechanical Testing, Electrical Conductivity Measurement.

Introduction

The AA7075 is one of the strongest aluminium alloys that have superior mechanical properties such as high strength-to-weight ratio, toughness, tensile strength etc. AA7075 finds application in the aerospace and automobile industries because of its natural ageing property. Also, aluminium alloys find wide applications in shipbuilding, marine structures etc. because of their lower corrosion rate [1]. When FSW and TIG welding processes are compared for AA6061-T6, the FSW joint shows higher strength compared to the TIG joint. The inferior mechanical properties in the case of TIG or metal inert gas welded (MIG) joint is due to the higher temperature generated during the process as compared to the FSW [2-8]. The mechanical properties of welded joints can be increased by using the FSW process rather than MIG. The heat-affected zone (HAZ) of the FSW joint is confined than the MIG process. In the FSW joint, electrical conductivity and hardness have a reciprocal effect [9]. In the case of FSW, hardness is lowest in HAZ, while in TIG and MIG welds hardness is lower in HAZ and weld centre [10]. When the corrosion behaviour of AA6061 alloy joined by FSW and TIG was compared, it was observed that in the case of FSW, the fine grain structure of the weld nugget zone caused corrosion. In the case of TIG, the corrosion is higher than both the parent material and FSW. This is because TIG weld contains plenty of silicon and aluminium eutectic precipitates at the dendrites of metal and inhomogeneous distribution of iron particles at these precipitates [11]. Joint made with TIG is sensitive to intergranular and exfoliation corrosion as compared to joints made with FSW and base metal AA5083-H321 [12]. In the case of AA6063-T6 joints, tensile strength is similar in both TIG and FSW joints before natural ageing [13]. AA2014 FSW has a lower corrosion rate as compared to welds made with TIG as the TIG weld zone consists of coarse grains [14]. Corrosion rate increases in the lower hardness region in the case of both TIG and FSW [14].

TIG welds with AA 4043 filler material showed higher hardness and corrosion resistance as compared to filler material AA4047 [18]. The appropriate value of current to perform TIG welding is 130 amperes [20]. The base metal AA5086-H116 showed a lower corrosion rate than samples with TIG and FSW welds. FSW joint showed better corrosion resistance to exfoliation, but FSW joint is susceptible to pitting corrosion in a contrast to TIG welds [21]. The lower thermal expansion coefficient of the Silicon and aluminium oxide layer causes discontinuity of the Al matrix which reduces the electron movement [23]. Friction stir vibration welding results in finer grains than FSW and TIG as a result of improved recrystallization [25].

Although many researchers compared FSW and TIG processes, investigation on the comparison of FSW with TIG in terms of

the corrosion behaviour and electrical conductivity of AA7075 is lacking. Thus, the aim of the current study is to compare the microstructure, mechanical, corrosion behaviour, and electrical conductivity properties of FSW and TIG welded AA7075 aluminium alloy. The results are compared in terms of microstructure, hardness, tensile properties, corrosion and electrical conductivity.

Material and Methods

Material

For the experimental study, the AA7075 rolled plates of 6 mm thickness were selected as the parent metal. With the help of a power hacksaw, the plates were cut to the desired size of 200 mm x 60 mm. Optical emission spectroscopy was used to identify the chemical composition of the base material. The composition of chemical elements and mechanical properties of AA7075 are shown in Table 1 and Table 2, respectively.

Table 1: The composition of chemical elements of AA7075 (Wt%)

Si	Fe	Cu	Mn	Mg	Cr	Zn	Al
0.3	0.35	1.5	0.11	2.4	0.22	5.5	Balance

Table 2: Mechanical and thermal properties of AA7075

Modulus of Elasticity (GPa)	Ultimate tensile strength (MPa)	Elongation (%)	Coefficient of Thermal Expansion [µm/m-0C]	Density (g/cm^3)	Rockwell hardness (HRB-B scale)
71.7	542	10%	23.6	2.81	87

Methods Adopted for Fabricating Joints

The trial and error experimental runs were performed and then FSW and TIG process parameters were selected to ensure defect-free joints. The longitudinal directions of the TIG and FSW welds were taken parallel to the rolling direction of AA7075. The abutting surfaces were cleaned before welding to ensure proper welding. In the case of TIG, a gap of 2 mm was left between the two plates being welded for filler material while in the case of FSW no gap was left. AA 4043-grade filler rod with a diameter of 2 mm was used for TIG welding. TIG welding was performed two-sided with a constant current of 110 and 122 ampere and with argon as shielding gas with a gas flow rate of approximately 16 L /min. The welding speed in the case of TIG was 150 mm/min. The voltage was 80 V.

As tool rotational speed increases the grain size also increases which ultimately results in lower tensile strength [24]. FSW was performed on the milling machine at optimal process parameters such as tool rotational speed and welding speed of 1000 rpm and 60 mm/min respectively. The tool used for FSW was made up of H13 with shoulder and a pin diameter of 18 and 6 mm respectively. The tool pin is characterized by left-hand threads with a 1 mm pitch and rotated in the counterclockwise direction. Fig. 1 shows a schematic of the FSW and TIG process. Fig. 2 show machines utilized for FSW and TIG process respectively.

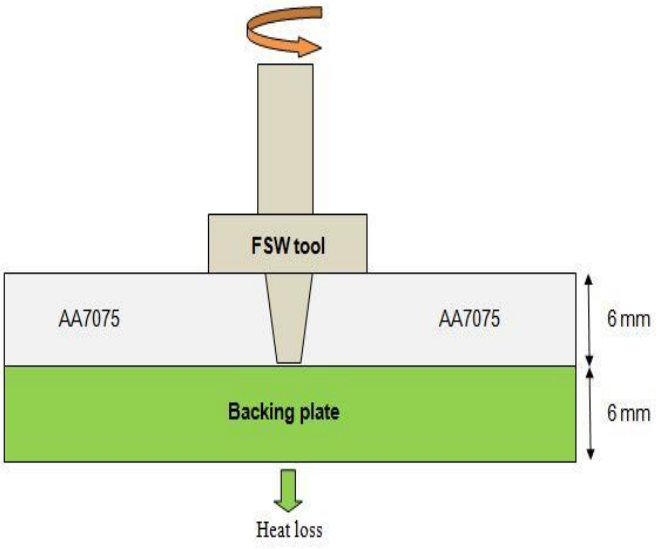

(a)

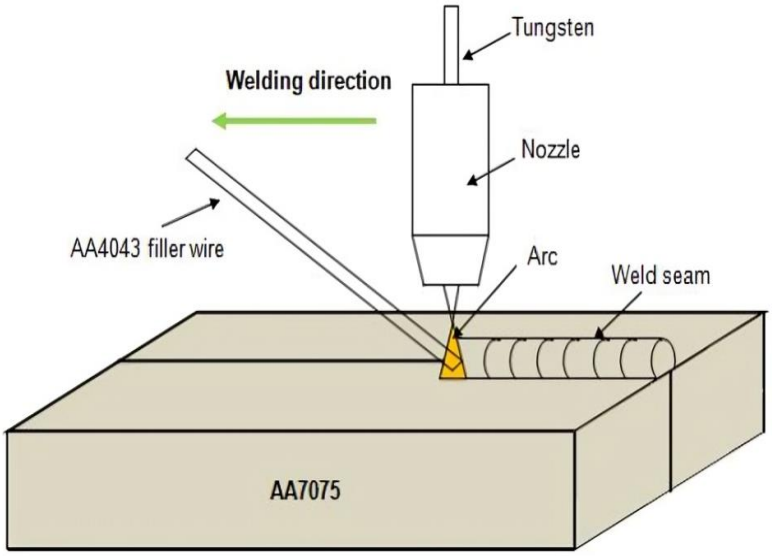

(b)

Figure 1: Schematic of (a) FSW process (b) TIG process

Figure 2: (a) Milling machine used for FSW (b) Machine used for TIG

Tests Performed on FSW and TIG Samples

Microstructure

For the microstructural study, samples were mounted and then polished by using Silicon Carbide papers of grades 600 to 1200, followed by polishing with a diamond paste of particle size1µm on a disc polishing machine. To reveal the microstructure, samples were etched using Keller's reagent (190 ml distilled water, 2 ml HF, 3 ml HCL and 5 ml HNO3). The time of the etching was 30 seconds. Using a light optical microscope a microstructural study was performed.

Exfoliation Corrosion

Aluminium forms a thin protecting film of Al2O3 which breaks in corrosive conditions. The exfoliation corrosion susceptibility of samples was conducted by preparing a test solution containing 4 M NaCl, 0.5M KNO3, and 0.1 M HNO3 in 1 litre of distilled water. The solution for the Exfoliation-Corrosion (EXCO) test was prepared as per ASTM G34-01 having an initial pH of approximately 0.4. Weight loss measurements were used to estimate the corrosion resistance of the samples. After 96 hours of immersion, the corroded samples were cleaned with nitric acid and dried up. The difference between the weight of the sample before and after the EXCO test provides the details about the loss of weight in grams [26]. Two samples were selected for the corrosion test of each welding process, and their corrosion rates are tabulated in Table 3.

The corrosion rate of samples was calculated as per ASTM G-1.

Corrosion rate (mm/year) = (KxW)/(AxTxD) (Eq 1)

Where A represents the total surface area of samples in cm^2, D is the material's density, T is the immersion time in hours, and the value of constant K is 8.76 X 10^4 mm/year.

Mechanical testing and Electrical Conductivity Measurement

Rockwell hardness test was used to measure hardness perpendicular to the welding direction using a ball indenter. The samples for hardness testing were prepared with a size of 20 mm width. The measurements were done on the top surface of the weld joint.

The tensile test specimens were tested according to ASTM E8 M-04. The tensile test was performed on a universal testing machine at a cross-head speed of 3mm/min at room temperature. The ultimate tensile strength (UTS) and percentage of elongation (%E) were evaluated. Fig. 3 shows a schematic of the tensile test sample. As per ASTM E1004-09, electrical conductivity tests were performed at the same locations as those for the hardness test. Fig. 4 shows the setup for the electrical conductivity measurement.

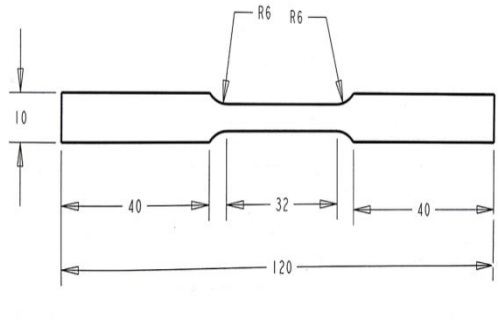

Figure 3: Schematic of tensile test sample

Figure 4: Setup for electrical conductivity measurement

Two samples were selected for corrosion, hardness, tensile test and electrical conductivity measurement and then average values were taken.

Results and Discussion

Microstructure

The grain size determines the severity of exfoliation corrosion. Elongated grains and coarse grain causes exfoliation corrosion. The severity of exfoliation corrosion increases with the increase in grain size [22]. There is no corrosive attack in the stir zone of the FSW joint as the stir zone consists of fine and equiaxed grains as shown in Fig. 5d. The average grain size of the FSW stir zone was 25µm, while the average grain size of the base metal was 95µm. The average grain size of HAZs of TIG and FSW were 80µm and 48µm respectively.

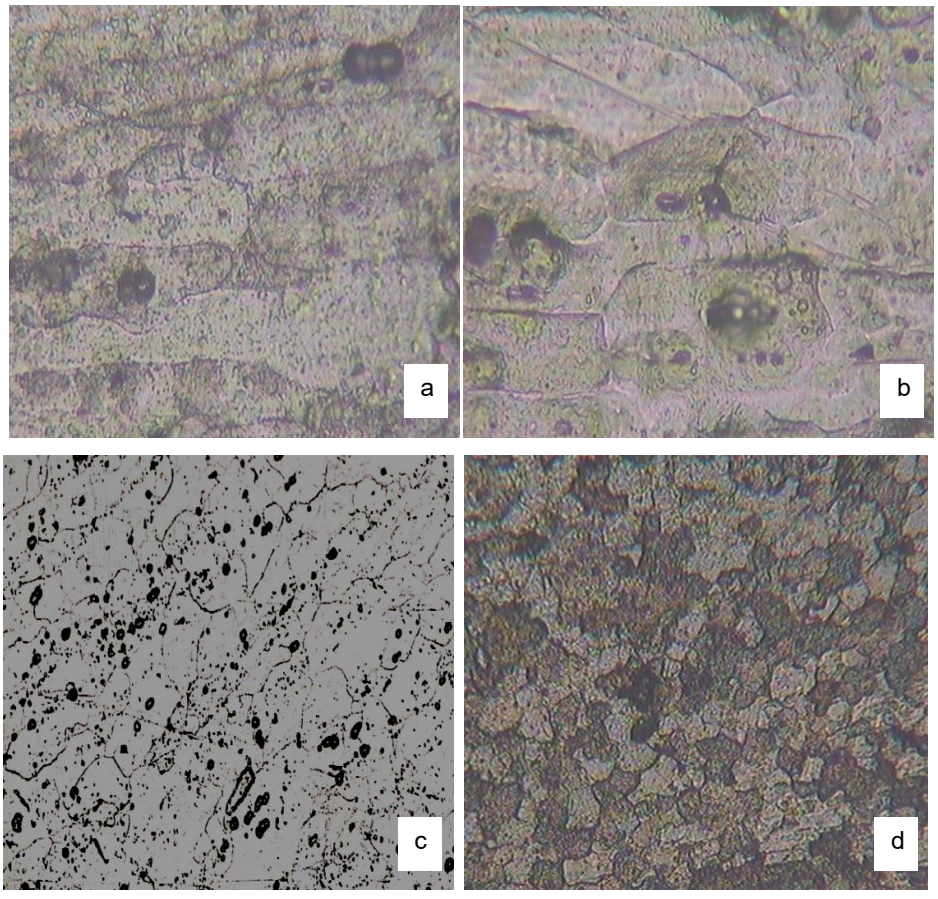

Figure 5: Optical microstructure (a) base metal, (b) TIG heat affected zone, (c) FSW heat affected zone, (d) FSW stir zone

Exfoliation Corrosion (EXCO) Test

During the EXCO test, the pH value of the solution increases from an initial value of 0.4 to approximately 3.5 due to the hydrolysis of aluminium ions. After immersing samples in EXCO solution, within 30 minutes bubbles started to form and there is a of foam on the top surface of the EXCO solution. Bubble **a** formation indicates the reaction of the aluminium oxide layer with Oxygen. Corrosion attack retards after 90 hours of immersion. The rise in the pH value of the EXCO solution reduces the corrosion attack. After the completion of 96 hours, corroded samples were taken out of the EXCO solution. The EXCO solution removes part of the material from the samples which were found to be loosely attached to samples as well as deposited at the bottom of the vessel [26].

From Table 3, it is clear that the corrosion rate is highest in the parent metal AA7075. The corrosion in the parent material is due to the galvanic corrosion of the copper with the aluminium [15]. Intergranular corrosion has been observed in the base metal. The pitting corrosion attack is more severe in the HAZ of TIG welded joints as compared to FSW welded joints as the grain size of HAZ of TIG contains coarse grains (80µm) as compared to the HAZ of FSW joints (48 µm). Corrosion attack is higher in the HAZ of TIG joints and there is no corrosion in the weld region. In the case of TIG filler material, AA4043 contains plenty of silicon which results in an increase in silicon concentration in the weld fusion zone. High silicon content in the weld region of TIG joints, results in a lower corrosion rate. Fig. 6 and 7 show samples before and after corrosion respectively.

Figure 6: Samples before corrosion test

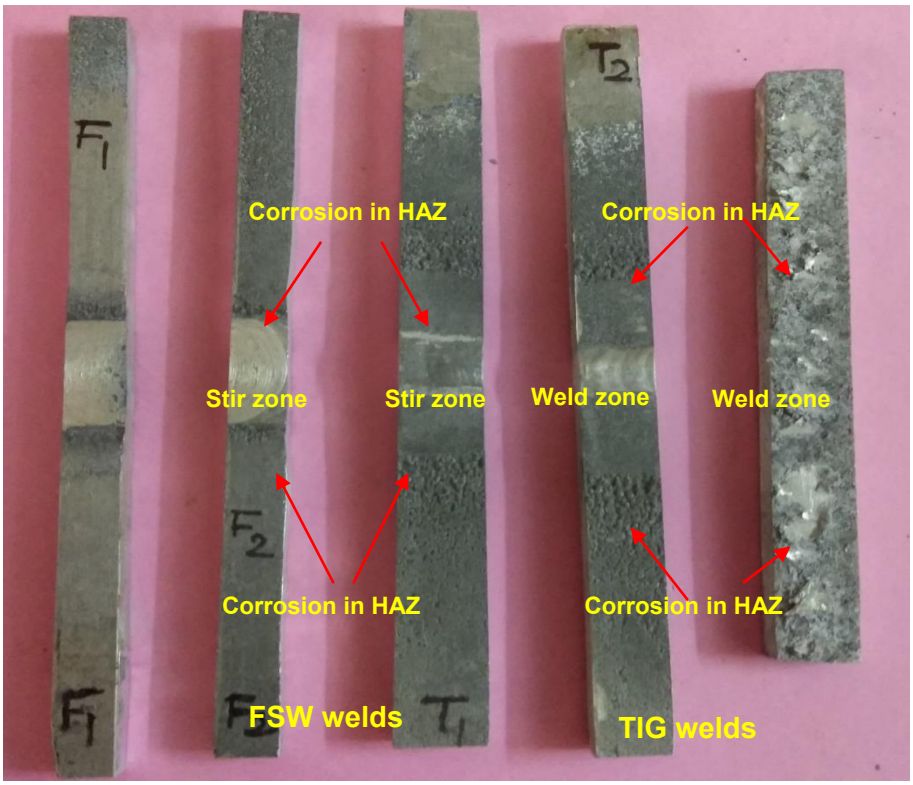

Figure 7: Samples after corrosion Corrected **labeling** in the image. Eg: FSW welds, TIG welds, Base metal etc.

Table 3: Corrosion rate of samples

Process	Sample No	Corrosion rate (mm/year)
TIG	T1	10.738
	T2	9.736
Parent metal	PM	18.21
FSW	F1	8.76
	F2	5.033

Hardness

The hardness of base metal is 87 HRB. In FSW, hardness value decreases in the weld nugget zone. In FSW, although drop in hardness has been noticed at the HAZ (about 65HRB), due to fine grain structure in the weld stir zone, the hardness recovers in this region and increases to 78 HRB which is 90% of hardness of the parent material. In joint fabricated with TIG, drop in hardness has been observed in weld center due to excessive heat and use of lower hardness AA4043 filler metal which causes softening of weld material and it is 46.5 HRB. This hardness is 54% of that of base metal. Also, AA 4043 filler material contains very few strengthening precipitates than the parent metal [3]. Fig. 8 shows the hardness distribution over the weld cross section of TIG and FS welded AA7075.

From Fig. 8, it is clear that FSW results in higher hardness than TIG at all locations of the sample.

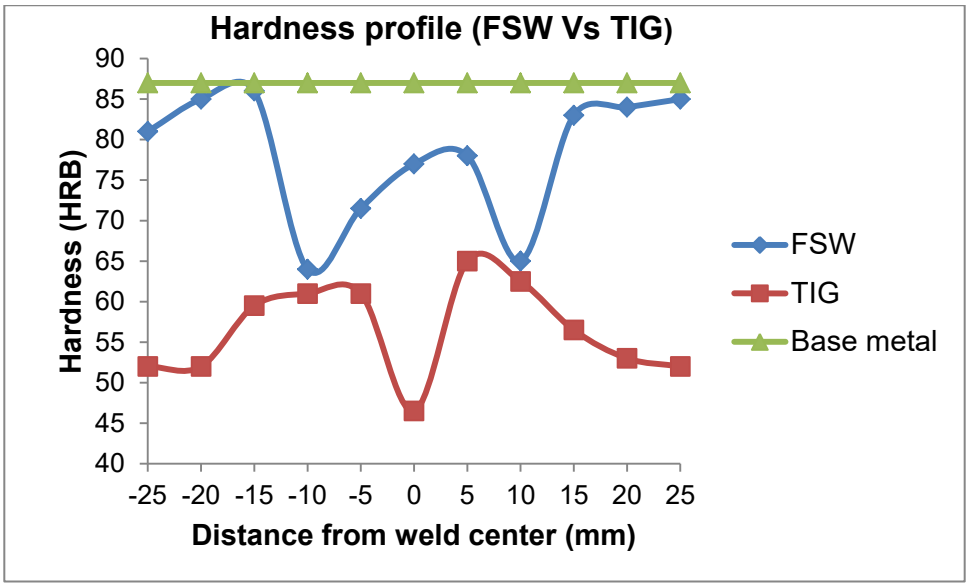

Figure 8: Hardness profile FSW Vs TIG

Comparison of Hardness Vs Electrical Conductivity

FSW Process

In the case of FSW, electrical conductivity and hardness showed a reciprocal effect, i.e. if hardness increases electrical conductivity decreases and vice versa. Therefore, electrical conductivity and hardness are non-linear to each other and hence hardness test can be replaced by non-destructive testing such as electrical conductivity (E) measurement. Hardness (H) Vs electrical conductivity graphs for weld cross-section of FSW and TIG are shown in Fig. 9 and 10 respectively.

From Fig. 9, it is clear that electrical conductivity has been increased in the HAZ and TMAZ of the FSW joint, and decreased in the weld stir zone. As a result of the thermo-mechanic process in the FSW, TMAZ experiences precipitate dissolution and has coarse grains. The grain boundaries that resist the mobility of electrons decrease as grain size increases. As a result, the mobility of electrons is improved, and electrical conductivity increases in TMAZ and HAZ. Because of the small grain size in the FSW weld stir zone, grain boundaries that oppose the mobility of electrons increase [26]. As a result, electrical conductivity is reduced in the weld nugget region [16,17]. From Fig. 9 it is clear that when hardness increases, electrical conductivity decreases and vice versa.

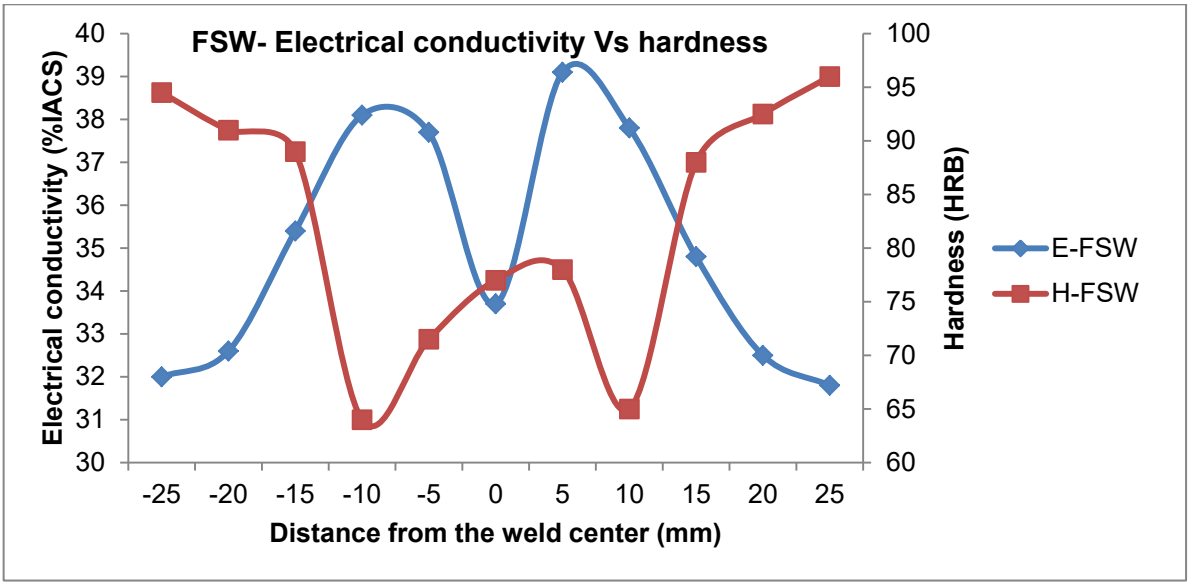

Figure 9: FSW electrical conductivity Vs hardness

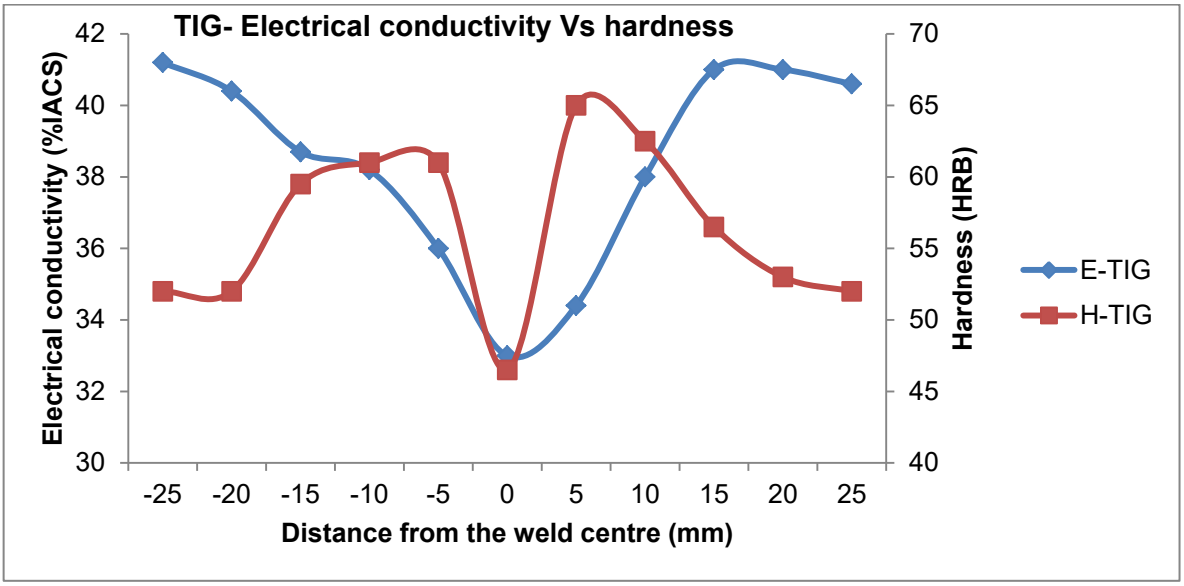

Figure 10: TIG electrical conductivity Vs hardness

TIG Process

In the case of TIG, no relation was found between hardness and electrical conductivity as shown in Fig. 10.

The electrical conductivity decreases as Silicon content increases. As TIG filler material AA4043 consist of 5-6% Silicon, electrical conductivity significantly reduces in the weld region. The lower thermal expansion coefficient of the Silicon and aluminium oxide layer causes discontinuity of the Al matrix which reduces the electron movement [23].

Ultimate Tensile Strength & % Elongation

From Table 4 it is clear that FSW results in higher strength and % elongation as compared to TIG. The TIG sample failed in the weld centre which is the lowest hardness region, while the FSW sample failed in the TMAZ of the weld region. In the case of the FSW joint, there is a significant difference between the microstructure of the stir zone and TMAZ which consist of coarse grains, the intersection between the stir zone and TMAZ becomes the weakest region and therefore tensile test sample of FSW failed at this intersection. The ultimate tensile strength (UTS) of FSW weld is 82.65% of that of base metal while the UTS of TIG is only 22.14% of that of base metal.

Table 4: Ultimate tensile strength and % elongation

Process	Ultimate tensile strength (UTS)	% elongation
FSW	448	7
TIG	120	5
Base metal	542	10

Conclusions

The microstructure strongly affects the mechanical, corrosion as well as electrical conductivity properties of TIG and FSW joints.

The grain size determines the severity of exfoliation corrosion. Elongated grains and coarse grain causes exfoliation corrosion. The severity of exfoliation corrosion increases with the increase in grain size.

Corrosion attack is predominant in HAZs in both TIG and FSW joints due to coarse grains. While there is no corrosion attack at the weld centre of FSW due to fine grains and high silicon content of filler material in the case of the TIG weld. The rate of corrosion can be ordered as Base metal > TIG > FSW.

Intergranular corrosion has been observed in the base metal.

Electrical conductivity and hardness are non-linear to each other in the case of friction stir welded joints, i.e., as hardness increases electrical conductivity decreases. Hence, the hardness test can be replaced by non-destructive testing such as electrical conductivity measurement. In the case of TIG, no relation was found between hardness and electrical conductivity.

Coarse grains are favourable for increasing electrical conductivity. TMAZ and HAZ of the FSW joint consist of coarse grains and have high electrical conductivity. Due to fine grains in the stir zone of the FSW joint as compared to other regions, the stir zone shows lower electrical conductivity.

High Silicon content at the weld region of TIG significantly reduces electrical conductivity.
The FSW joints result in improved corrosion resistance and mechanical properties as compared to welds with the TIG.

Funding: This work is not funded by any agency.

Declarations

Conflict of interest: The authors declare that they have no known competing financial interests or personal relationships that could have appeared to influence the work reported in this paper.

References

1. Kumar K.; Kailas S.: The role of friction stir welding tool on material flow and weld formation. Mater Sci Eng A. 485, 367-374 (2008). https://doi.org/10.1016/j.msea.2007.08.013
2. Shukla R.; Shah P.: Comparative study of friction stir welding and tungsten inert gas welding process. Indian J Sci Technol. 3, 667-671 (2010) .DOI: 10.17485/ijst/2010/v3i6.17
3. Thakur N.; Lal H. : Experimental comparison of TIG and friction stir welding processes for aluminium 6063-T6. Int J of Emerg Technol. 6(2), 189-194 (2015).
4. Patil C.; Patil H.: Experimental investigation of hardness of FSW and TIG joints of aluminium alloys of AA7075 and AA6061. Frat Integrita Strutt. 10 (37), 325-332 (2016). DOI:10.3221/IGF-ESIS.37.43
5. Anjaneya P.; Prasanna P.: Experimental comparison of the MIG and friction stir welding processes for AA6061 aluminium alloy. Int J of Min Metall Mech Eng. 1, 137-140 (2013).
6. Kumar A.; Gautam S.: Heat input and joint efficiency of three welding processes TIG, MIG and FSW using AA6061. Int J Mech Eng Robot Res. 1, 89-94 (2014).
7. Kulekci M.; Kaluc E.; Sik A.; Basturk O.: Experimental comparison of mig and friction stir welding processes for en AW 6061-T6 aluminium alloy. Arab J Sci Eng. 35, 323-330 (2010).
8. Kumar R.; Kumar G.; Roy A.; Sinha R.: A comparative analysis of friction stir and tungsten inert gas dissimilar AA5082-AA7075 butt welds. Materials Science for Energy Technologies. 5, 74-80 (2022). https://doi.org/10.1016/j.mset.2021.12.002
9. Ghodwade S.; Patil S.; Gogte C.: Experimental study of MIG welding and solid state welding for age hardenable AA7075 aluminium alloy. Int J Mech Eng. 3, 46-52 (2015).
10. Yeni C.; Sami S.; Pakdil M.: Comparison of mechanical and microstructural behavior of TIG, MIG and friction stir welded 7075 aluminium alloy. Kovove Materialy. 47 (5), 341-347 (2009).
11. Fahimpour V.; Sadrnezhaad S.; Karimzadeh F.: Corrosion behavior of aluminium 6061 alloy joined by friction stir welding and gas tungsten arc welding methods. Mater Des. 39, 329-333 (2012). https://doi.org/10.1016/j.matdes.2012.02.043
12. Grover H.; Chawla V.; Gurbhinder Brar G.: Comparing mechanical and corrosion behaviour of TIG and FSW weldments of AA5083-H321. Indian J Sci and Technol. 10(45), (2017) DOI:10.17485/ijst/2017/v10i45/113537
13. Khanna N.; Choudhary B.; Airao J.: Experimental comparison of TIG and friction stir welding process for AA6063-T6 aluminium alloy. Proceedings of ICIIF. (2018). DOI:10.1007/978-981-13-1966-2_56
14. Sinhmar S.; Dwivedi D.: A study on corrosion behavior of friction stir welded and tungsten inert gas welded AA2014 aluminium alloy. Corros Sci. 133, 25-35 (2018) https://doi.org/10.1016/j.corsci.2018.01.012
15. Rao T.; Reddy G.; Rao G.: Studies on salt fog corrosion behavior of friction stir welded AA7075-T651 aluminium alloy. Int J of Mater Res. 105, 375-385 (2014) DOI:10.3139/146.111033
16. Santos T.; Vilaca P.; Miranda R.: Electrical conductivity field analysis for evaluation of FSW joints in AA6013 and AA7075 alloys. J Mater Process Technol. 211,174-180. (2011). https://doi.org/10.1016/j.jmatprotec.2010.08.030
17. Santos T.; Vilaca P.; Miranda R.: Microstructural mapping of friction stir welded AA7075-T6 and AlMgSc alloys using electrical conductivity. Sci Technol Weld Join. 16, 630-635 (2011). DOI:10.1179/1362171811Y.0000000052
18. Shah L.; Razak N.; Juliawati A.: Investigation on the mechanical properties of TIG welded AA6061 alloy weldments using different aluminium fillers. Int J Eng Technol. 2, 116-119 (2013). DOI:10.5176/2251-3701_2.2.81
19. HE Zhen-bo.; Yong-yi P.; Zhi-min Y.; Xue-feng L.: Comparison of FSW and TIG welded joints in Al-Mg-Mn-Sc-Zr alloy plates. Trans Nonferrous Met Soc China. 21, 1685-1691 (2011). https://doi.org/10.1016/S1003-6326(11)60915-1
20. Dakave U.; Patil S.; Shah A.: Comparative analysis of FSW and TIG welding processes for joining dissimilar aluminium alloys AA6082-AA1100 based on multi response opti-

mization using Entropy-Topsis approach. Int J Adv Res Eng Technol. 12(1), 617-630 (2021).https://doi.org/10.34218/IJARET.12.1.2020.056
21. Hans V.; Bajwa P.: Comparison of mechanical and corrosion behavior of aluminium alloy weldments. Int J Res App Sci Eng Technol. 6(3), 2900-2906 (2018).
22. McNaughtan D.; Worsfold M.; Robinson M.: Corrosion product force measurement in the study of exfoliation and stress corrosion cracking in high strength aluminium alloys. Corros Sci. 45(10), 2377-2389 (2003). https://doi.org/10.1016/S0010-938X(03)00050-7
23. Cao R.; Jiang J.; Wu C.: Effect of addition of Si on thermal and electrical properties of Al-Si-Al2O3 composites. IOP Conf. Series: Mater. Sci. Eng. 213, (2017) doi:10.1088/1757-899X/213/1/012001
24. Dwivedi U, Tiwari S, Mishra A, Das S. Comparative study of weld characteristics of Friction stir welded joints on aluminium 7075 with autogenous TIG. Mater.Today: Proc. 2020; 22: 2532-2538
25. Bagheri B, Abbasi M, Abdollahzadeh A. Microstructure and mechanical characteristics of AA6061-T6 joints produced by friction stir welding, friction stir vibration welding and tungsten inert gas welding: A comparative study. Int. J. Miner. Metall. 2021; 28(3): 450-461.
26. Kulkarni B, Pankade S, Tayde S, Bhosle S. Corrosion and mechanical aspects of friction stir welded AA6061 joints: Effects of different backing plates. J. Mater. Eng. Perform. 2023. https://doi.org/10.1007/s11665-023-07900-x